J Mater Sci (2007) 42:5299–5306
DOI 10.1007/s10853-007-1771-y

Preparation of surfactant templated nanoporous silica spherical particles by the Stöber method. Effect of solvent composition on the particle size

Naoki Shimura · Makoto Ogawa

Received: 29 November 2005 / Accepted: 6 November 2006 / Published online: 19 May 2007

Abstract Monodispersed nanoporous silica spherical particles with the particle size ranges from 0.01 μm to 1.5 μm were successfully prepared by the Stöber method combined with supramolecular templating approach. The particles formed from homogeneous solutions containing tetraethoxysilane, cetyltrimethylammonium chloride, methanol, and aqueous ammonia solution at room temperature. In the present study, methanol/tetraethoxysilane ratio was the factor to control the particle size. With increasing the methanol/tetraethoxysilane ratios from 1,125 to 6,000, particle size decreased from 1.5 μm to 0.01 μm. The calcination of the particles resulted in the spherical porous silicas with the average pore sizes of around 2.0 nm irrespective of the particle size. The particle morphology retained after the calcination.

Introduction

After the discovery of nanoporous silicas prepared by supramolecular templating approach, there have been so many reports on the nanostructure, chemical composition, morphology as well as the applications of the nanoporous silicas and related surfactant templated materials [1–6]. Since the morphology is a key issue for the certain kind of application, the preparation of nanostructured and nanoporous silicas in such controlled morphologies as films [7, 8], fibers [9, 10], and monoliths [11] has been actively investigated. Particle morphology from simple ones (plate [12] and sphere [13–39]) to complex ones (such as spiral and gyroid) [40–45] of nanoporous silicas has also attracted much attention.

Among reported particle morphology, spherical particle of controlled size is one of the most attractive one because of their possible uses for chromatography, optics and so on [13, 14]. Accordingly, nanoporous silica spherical particles have been prepared by utilizing various synthetic approaches including those based on emulsion chemistry [15] and using morphology template [16], and spraying [17–22]. The Stöber method, which was developed for the preparation of monodispersed silica spherical particles with controlled size [46–48], has been successfully applied to prepare surfactant templated nanoporous silica spherical particles [23–37]. The nanoporous silica spherical particles with the particle size from 0.06 μm to 2.3 μm with relatively narrow particle size distribution have been obtained so far. For this kind of synthesis, a wide variety of experimental parameters such as chemical compositions and silica precursor are known to affect the particle size [23, 25, 27–29, 31, 33, 37]. However, it is still difficult to directly correlate the particle size and an experimental parameter. In addition, there remain synthetic challenges toward larger particles, narrower particle size distribution, controlled pore size and so on. In the present paper, we report the preparation of surfactant templated nanoporous silica spherical particles with the particle size from 0.01 μm to 1.5 μm and narrow particle size distribution. The particle size was sequentially controlled by simply changing the methanol/tetraethoxysilane in the starting solution.

N. Shimura · M. Ogawa (✉)
Graduate School of Science and Engineering, Waseda University, Nishiwaseda 1-6-1, Shinjuku-ku, Tokyo 169-8050, Japan
e-mail: makoto@waseda.jp

M. Ogawa
Department of Earth Sciences, Waseda University, Nishiwaseda 1-6-1, Shinjuku-ku, Tokyo 169-8050, Japan

Experimental

Materials

Tetraethoxysilane (abbreviated as TEOS) and cetyltrimethylammonium chloride (abbreviated as CTAC) were obtained from Tokyo Kasei Kogyo Co., Ltd. and were used without further purification. Methanol and 28% aqueous ammonia solution were reagent grade of Kanto Chemical Co., Inc.

Sample preparation

Synthetic procedures are similar to our reported ones [37]. A typical synthetic procedure is as follows: CTAC (0.211 g), deionized water (17.7 g), methanol (100 mL), and 28% aqueous ammonia solution (7.2 g) were mixed in a sealed vessel and the solution was shaken for 15 s at room temperature. To which solution was added TEOS (0.368 mL) and then the mixture was shaken for 3 s. The mixture was aged at room temperature for 20 h. The molar ratio of TEOS:CTAC:water:methanol :ammonia was 1:0.4:774:1501:72. The solution became turbid after the reaction for ca. 10 min, indicating particle formation. After the aging, products were separated by centrifugation (25,000 rpm, 20 min). The products were washed with methanol and were dried at 60 °C for a day. Surfactant removal was conducted by calcination in air at 550 °C for 10 h at a heating rate of 150 °C h^{-1}. In order to investigate the effects of the chemical composition in the starting solution on the particle size, amount of the methanol was varied: molar methanol/TEOS ratios = 300 (methanol = 20 mL), 750, 1,125, 1,500, 1,875, 2,250, 2,625, 3,000, 3,750, 4,500, 5,250, and 6,000 (methanol = 400 mL). In each case, the ammonia concentration was fixed (1 mol L^{-1}) by adjusting the amount of the 28% aqueous ammonia solution (TEOS/water ratios was also fixed). When the methanol/TEOS ratios were 5,250 and 6,000, the preparation was also conducted by the aging for 120 h.

Characterization

Scanning electron micrographs (SEM) were obtained on a Hitachi S-2380N scanning electron microscope. Prior to the measurements, the samples were coated with gold. Particle size distributions and average particle sizes were obtained by SEM observation for no less than 200 primary particles. Field Emission scanning electron micrographs (FE-SEM) were obtained on a Hitachi S-5200 scanning electron microscope. Prior to the observation of the cross-section, the calcined particles were crushed. Transmission electron micrographs (TEM) were obtained on a JEOL JEM-100CX transmission electron microscope. Thermogravimetric-differential thermal analysis (TG-DTA) curves were recorded on a Rigaku TG-8120 instrument at a heating rate of 3 °C min^{-1} and using α-alumina as the standard materials. In the present paper, silica yield means the atomic ratio of Si in the particles to Si in the added TEOS. The silica yields were determined from corrected product weight and the TG-DTA of the as-synthesized particles by our reported method [37]. X-ray diffraction (XRD) was performed on a RAD IB diffractometer (Rigaku) using monochromatic Cu Kα radiation, operated at 40 kV and 20 mA. The nitrogen adsorption/desorption isotherms of the particles were measured at –196 °C on a Belsorp 28SA instrument (Bel Japan Inc.). Prior to the measurements, the as-synthesized and calcined samples were dried at 80 and 120°C under vacuum for 3 h, respectively.

Results and discussion

When the syntheses were conducted at the methanol/TEOS ratios of 300–4,500, white blocks were obtained after the centrifugation. The white blocks easily broke up into powders without any mechanical stress. The product prepared at the methanol/TEOS ratio of 5,250 for 20 h was transparent monoliths. The monoliths were mechanically hard if compared with the white blocks. When the methanol/TEOS ratio was 6,000 and aging time was 20 h, the product was not obtained.

The particle morphology was microscopically examined using SEM (Fig. 1). Both white blocks and monolith were composed of small particles (mainly spherical). When the methanol/TEOS ratio was 300, particles with irregular morphology including ellipsoidal ones were observed in addition to the spherical particles in the SEM image shown in Fig. 1a. The number of the particles with irregular morphology decreased as the methanol/TEOS ratios increased. When the methanol/TEOS ratios were 1,125–5,250, all the particles were spherical.

The SEM observations indicated that the particle size was smaller as the methanol/TEOS ratios increased from 1,125 to 3,000, as shown in Fig. 1. The particle size distributions of the calcined particles are shown in Fig. 2, and the average particle size, the standard deviation, and the coefficient of variations (standard deviation/average) are summarized in Table 1. When the synthesis was conducted at the methanol/TEOS ratios of 1,125–3,000, the particle diameter was changed from 1.5 μm to 0.18 μm without significant change of the particle size distribution. Thus, particle size was successfully controlled by changing the methanol/TEOS ratios in the starting solutions. The present approach resulted in the monodispersed spherical particles

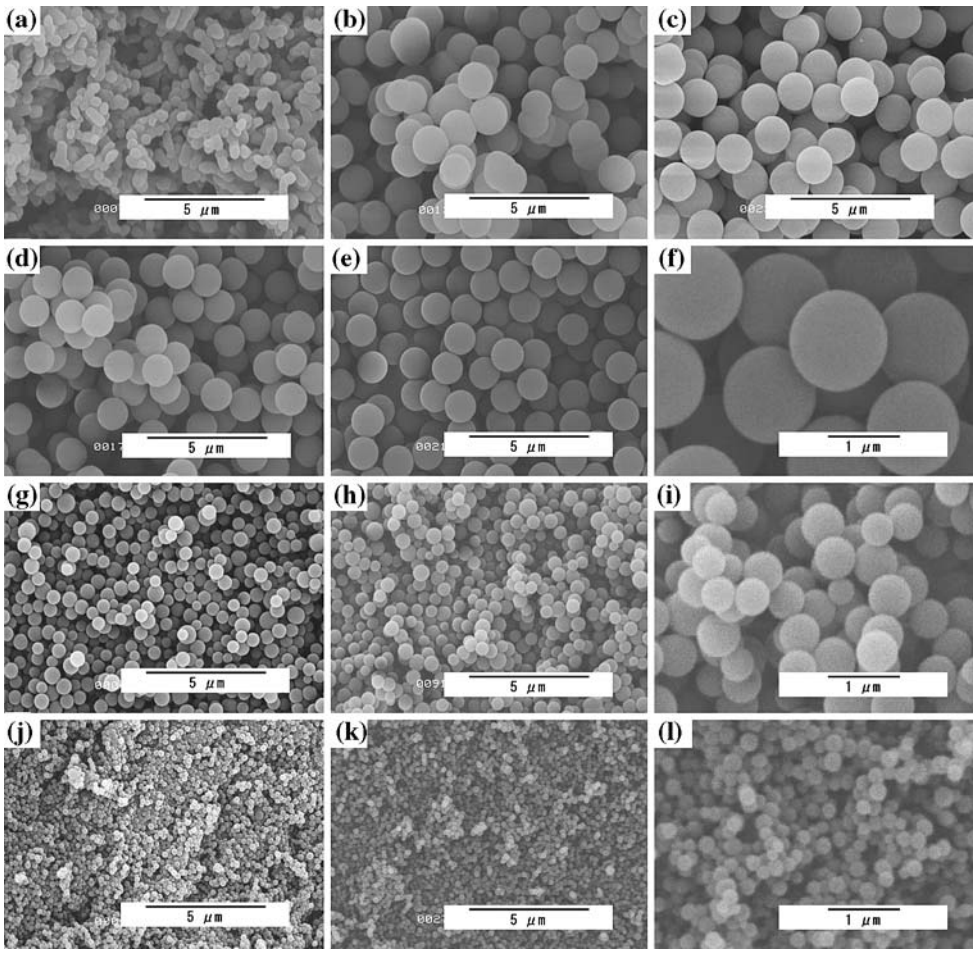

Fig. 1 SEM images of (**a–d**, **g**, **j**) the as-synthesized and (**e**, **f**, **h**, **i**, **k**, **l**) the calcined particles prepared at the methanol/TEOS ratios of (**a**) 300, (**b**) 750, (**c**) 1,125, (**d**, **e**, and **f**) 1,500, (**g**, **h**, and **i**) 2,250, and (**j**, **k**, and **l**) 3,000. Figure (**f**), (**i**), and (**l**) are close up views of Figure (**e**), (**h**), and (**k**), respectively

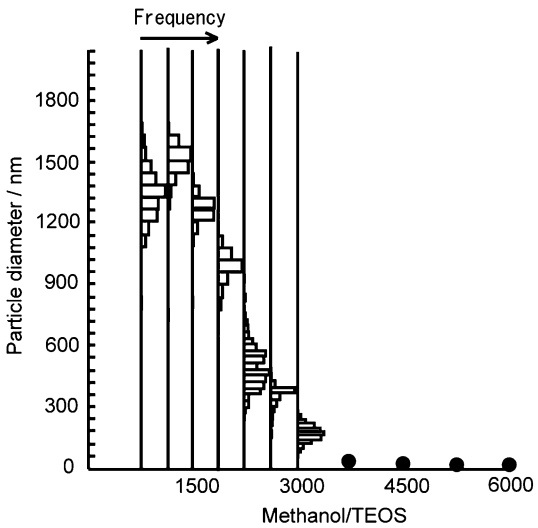

Fig. 2 Particle size distributions of calcined particles as a function of the methanol/TEOS ratios

in a wider size range if compared with those achieved in the reported examples (reaction time; 0.4–1.8 μm [37], chemical compositions; 0.08–0.8 μm [29], 0.06–0.7 μm [31], 0.5–1 μm [33]). The increase of methanol in the starting solution causes the decrease of the concentration of TEOS and CTAC, which are though to affect the reaction probably at the initial stage of precipitation. However, due to the complexity of the present system, it is difficult to explain the role of methanol to Si ratio on the particle size at present.

We have already reported the preparation of mesoporous silica spherical particles at 3 °C [37]. If compared with the particle size (1.75 μm) of the product obtained in the previous study (at the methanol/TEOS ratio of 1,500 and at 3 °C), the particle (1.29 μm) prepared from the solution of the same chemical composition at room temperature was smaller by 26%, showing that the synthetic temperature is a factor to control the particle size. Though the effects of the synthetic temperature are worth further investigating, we did not go to the problem in more detail in the present study and focused on the effect of the composition of the starting solution on the particle size in order to make discussion simple.

Figure 3 shows the TG-DTA curves of the as-synthesized particles prepared at the methanol/TEOS ratio of

Table 1 Average particle size, standard deviation, and coefficient of variations of calcined particles

Methanol/TEOS	Number of particles*	Average particle diameter/μm	Standard deviation/μm	Coefficient of variations/%
750	217	1.36	0.12	8.9
1,125	212	1.52	0.09	5.8
1,500	260	1.29	0.06	4.9
1,875	340	1.01	0.08	7.6
2,250	274	0.51	0.10	20.2
2,625	402	0.33	0.05	15.3
3,000	400	0.18	0.04	20.0

* Number of particles used for the particle size distribution

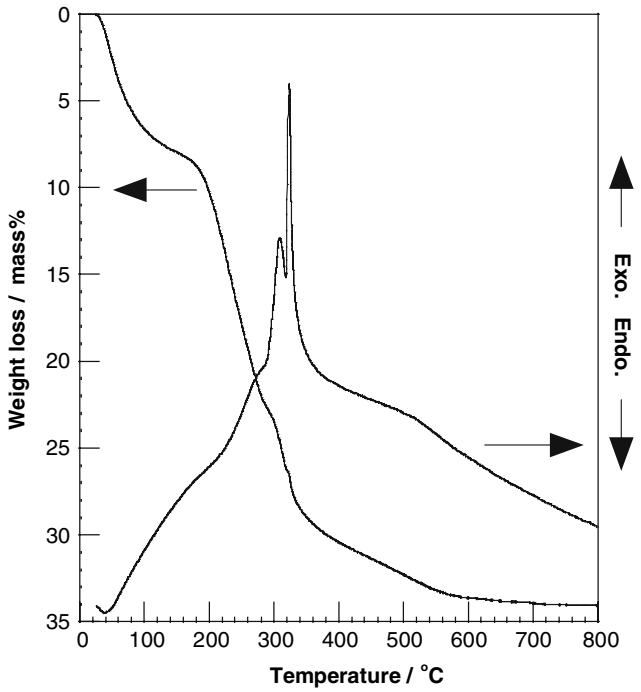

Fig. 3 TG-DTA curves of the particles prepared at the methanol/TEOS ratio of 1,500

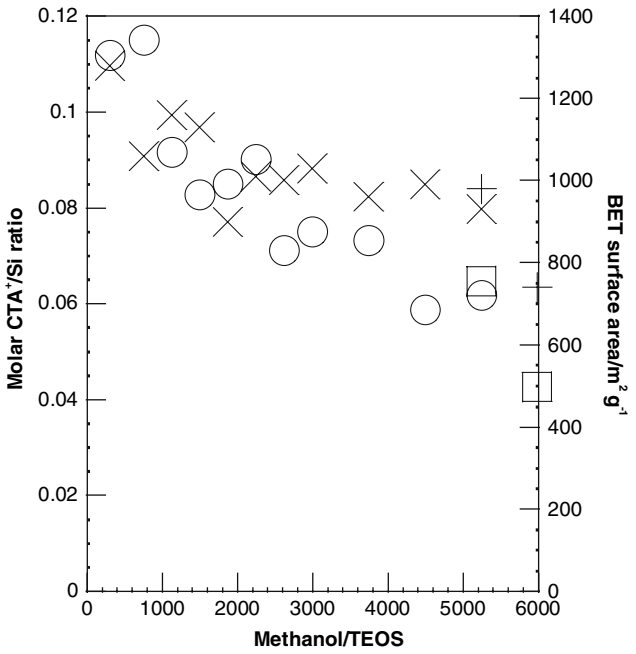

Fig. 4 CTA^+ contents of as-synthesized particles (circle) and BET surface areas (multiple) of calcined particles prepared by the aging for 20 h as a function of the methanol/TEOS ratios. Those of calcined particles prepared by the aging for 120 h were square and plus, respectively

1,500 as a typical example. The TG curves of the as-synthesized particles showed weight losses at around 150–650 °C. Since exothermic peaks were observed in the corresponding DTA curves, as shown in Fig. 3, the reaction was ascribed to the oxidative decomposition of CTA^+ [37, 49, 50]. The weight observed at 800 °C indicated the weight of the silica in the as-synthesized particles. The CTA^+/Si ratios were determined from these values [37]. Figure 4 shows the molar CTA^+/Si ratios of the as-synthesized particles as a function of the methanol/TEOS ratios. There is a general tendency toward smaller CTA^+ contents as the methanol/TEOS ratios increase.

When the methanol/TEOS ratios were 5,250 and 6,000, the aging time was prolonged to 120 h. As a result, the transparent hard monolith, as described before, was obtained though the product was not obtained when the preparation was conducted at the methanol/TEOS ratio of 6,000 by the aging for 20 h. The silica yield [37] of the product prepared with the methanol/TEOS ratio of 1,500 was ca. 100%. Those of the products prepared with the methanol/TEOS ratios of 5,250 by the aging for 20 h and 120 h was ca. 80% and 100%, respectively. In our separate study on the particle growth, the particle size increased as the silica yield was increased. Thus, the particle growth was slower as MeOH/TEOS ratios in the starting solutions increased.

Based on the above TG-DTA results, the as synthesized particles were calcined in air at 550 °C for 10 h in order to remove surfactant. The particle morphology was retained even after the surfactant removal, as revealed by the SEM observations. Figure 1e, f, h, i, k, and l shows the change in the particle morphology of the product prepared at the

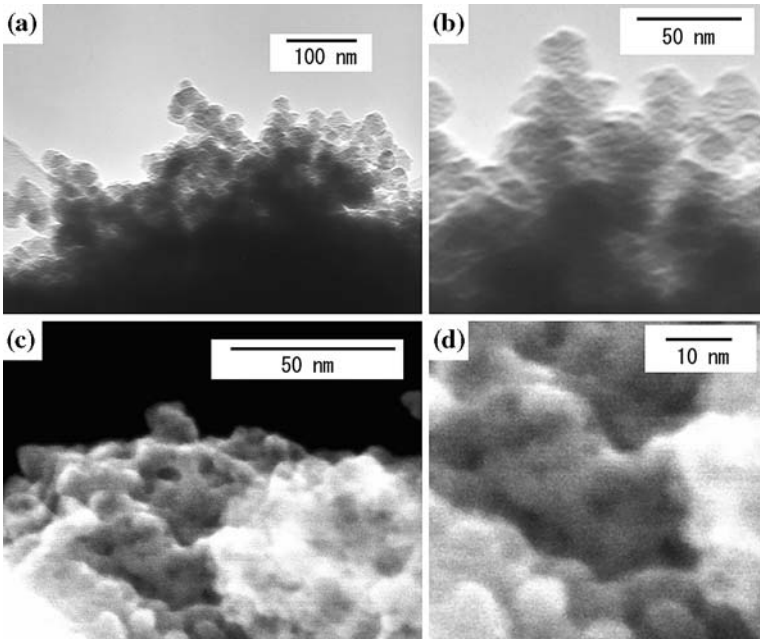

Fig. 5 TEM (**a** and **b**) and FE-SEM(**c** and **d**) images of the calcined particles prepared at the methanol/TEOS ratios of (**a** and **b**) 5,250 and (**c** and **d**) 6,000 for 120 h. Figure (**b**) and (**d**) are close up views of Figure (**a**) and (**c**), respectively

methanol/TEOS ratios of 1,500, 2,250, and 3,000 upon calcination. The average particle sizes of the as-synthesized and calcined particles prepared at the methanol/TEOS ratio of 1,500 were 1.30 (standard deviation = 0.08 μm) and 1.29 μm (standard deviation = 0.06 μm), respectively. The particle size did not change significantly for all the products prepared in the present study. The particle weight decreased (ca. 26% (methanol/TEOS = 1,500)) by the calcination due to the surfactant removal as shown in Fig. 3. On the other hand, the average particle size did not decrease significantly (only 1% (methanol/TEOS = 1,500)). These results indicated that the particle density became lower by the calcinations. Thus, the formation of nanopore after the surfactant removal was indicated.

Figure 5 shows the TEM and the FE-SEM images of the calcined products prepared at the methanol/TEOS ratios of 5,250 and 6,000 by the aging for 120 h. The particle diameter of these particles was 0.02 μm and 0.01 μm, respectively. The XRD patterns of the calcined particles are shown in Fig. 6. The XRD patterns showed single and broad peaks irrespective of the methanol/TEOS ratios, indicated the disordered mesostructures. The FE-SEM images of the particle surface and the cross-sectional view of the broken particles are shown in Fig. 7. The FE-SEM image shows the isolated spherical pore with regular size. Pores with the diameter of ca. 2 nm were observed at the particle surface and the cross-section (Fig. 7b and c)

XRD patterns of the calcined particles prepared at methanol/TEOS of (a) 300, (b) 1,500, (c) 4,500, and (d) 5,250.

Nitrogen adsorption/desorption isotherms of the particles prepared at the methanol/TEOS ratios of 1,500, 3,000, and 6,000 after the calcinations are shown in Fig. 8. All the calcined particles were nanoporous, irrespective of the particle size. BET [51] surface areas and BJH [52] pore size are summarized in Table 2. The pore size distributions were narrow for all the calcined products as shown in Fig. 9. The pore diameters were around 2 nm, irrespective of the particle size and were in agreement with the results of FE-SEM observations (Fig. 7).

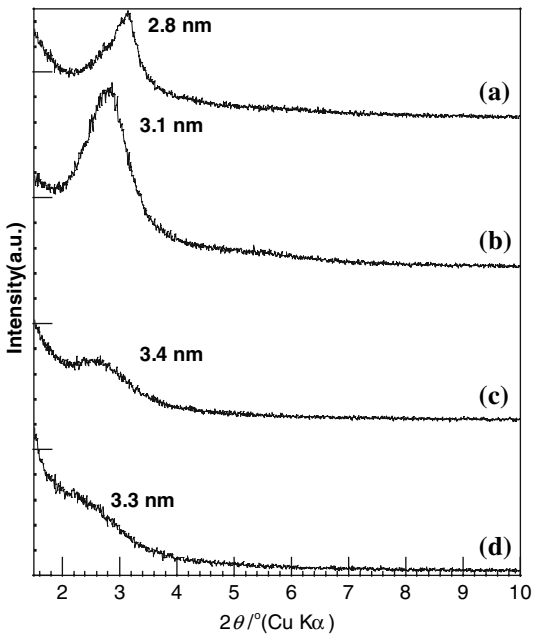

Fig. 6 XRD patterns of the calcined particles prepared at methanol/TEOS of (**a**) 300, (**b**) 1,500, (**c**) 4,500, and (**d**) 5,250 (120 h)

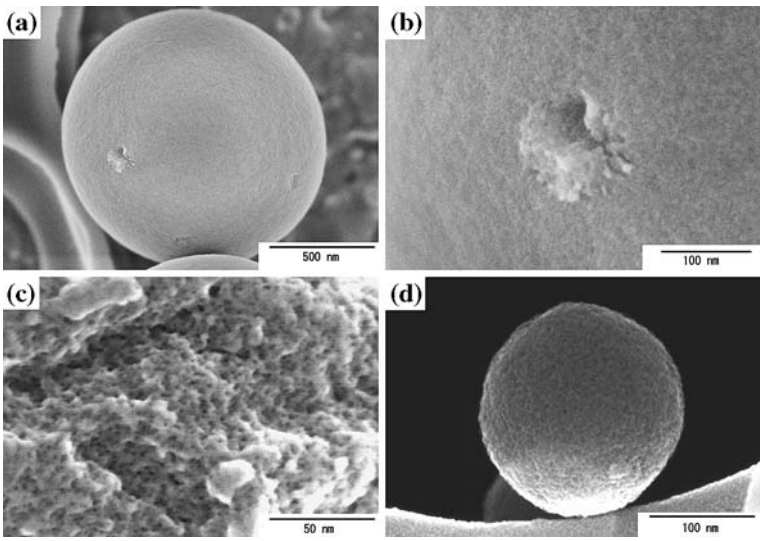

Fig. 7 FE-SEM images of calcined particles (methanol/TEOS = 1,500): (**a**) scarred particle, (**b**) close-up view of the scar and particle surface, and (**c**) cross-sectional view of a broken particle (methanol/TEOS = 1,500). FE-SEM image (**d**) was recorded for a calcined particle prepared at methanol/TEOS of 3,000

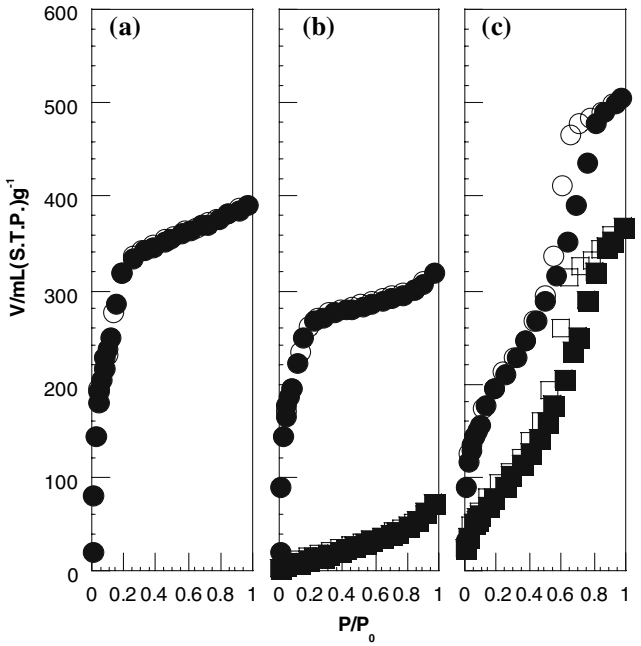

Fig. 8 Nitrogen adsorption/desorption isotherms of as-synthesized (square) and calcined (circle) particles. The particles were prepared at the methanol/TEOS ratios of (**a**) 1,500, (**b**) 3,000, and (**c**) 6,000 (120 h) (adsorption: filled symbol, desorption: opened symbol)

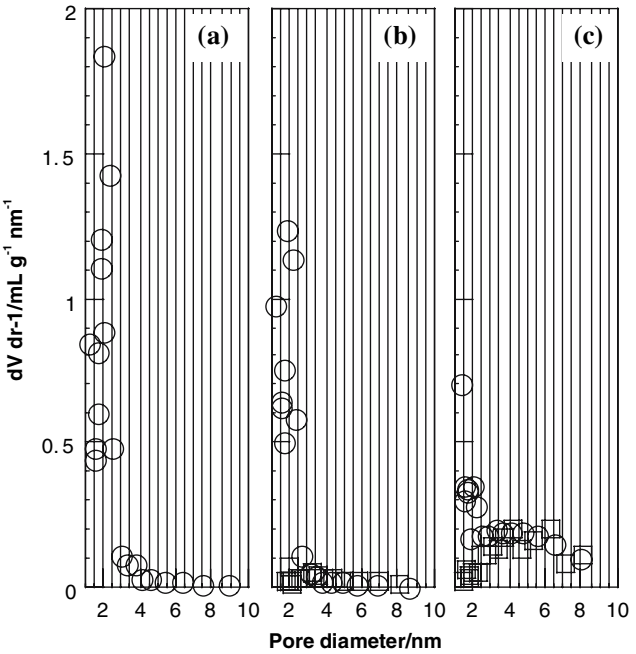

Fig. 9 BJH Pore size distribution of (square) the as-synthesized and (circle) the calcined particles prepared at the methanol/TEOS ratios of (**a**) 1,500, (**b**) 3,000, and (**c**) 6,000 (120 h)

When the methanol/TEOS of 5,250 and 6,000 (20 h and 120 h), the as-synthesized particles were also porous, as revealed by the nitrogen adsorption isotherms, as shown in Fig. 9c. For example, BET surface area of the as-synthesized particles prepared at methanol/TEOS of 6,000 for 120 h, as shown in Fig. 8c, was 320 $m^2 g^{-1}$. Since the particles are small (several ten of nm) as shown in Fig. 5, nitrogen was probably adsorbed at the inter-particle region. Sharp peaks at 2 nm were observed for the calcined particles. The pores with the diameter of 2 nm were made by the surfactant removal.

Particles with narrower size distribution and in a wider size range may be achieved by optimizing the reaction conditions. The variation of the pore size is another topic of interests. Efforts are being made in our laboratory for these problems and the results will be reported subsequently.

Conclusions

Nanoporous silica spherical particles with the pore size of 2 nm were prepared by the Stöber method in the presence

Table 2 Particle diameter, standard deviation, BET surface area, and pore diameters of the calcined particles as a function of the methanol/TEOS ratios in starting solutions

Methanol/TEOS	Particle diameter/μm	Standard deviation/μm	Surface area/m^2 g^{-1}	Pore diameter/nm
300	0.5	-	1,280	1.9
750	1.36	0.12	1,060	2.0
1,125	1.52	0.09	1,160	2.1
1,500	1.29	0.06	1,130	2.1
1,875	1.01	0.08	900	2.1
2,250	0.51	0.10	1,010	2.0
2,625	0.33	0.05	1,000	1.9
3,000	0.18	0.04	1,030	2
3,750	0.04	–	960	1.9
4,500	0.03	–	990	1.9
5,250 (aging for 20 h)	–*	–	930	1.9
5,250 (aging for 120 h)	0.02	–	980	2.1
6,000 (aging for 120 h)	0.01	–	740	2.0

* Microscopy observation was not conducted

of cetyltrimethylammonium chloride. The particle size was successfully controlled from 0.01 μm to 1.5 μm by simply changing the composition of the staring solutions.

Acknowledgement This work was supported by a Grant-in-Aid for Scientific Research on Priority Areas (417) from the Ministry of Education, Culture, Sports, Science and Technology (MEXT) of the Japanese Government. Waseda University (as a special research project) and Tokuyama Science and Technology Foundation also supported us financially.

References

1. Stein A, Melde BJ, Schroden RC (2000) Adv Mater 12:1403
2. Sayari A, Hamoudi S (2001) Chem Mater 13:3151
3. On DT, Desplantier-Giscard D, Danumah C, Kaliaguine S (2001) Appl Catal A 222:299
4. Taguchi A, Schüth F (2005) Microporous Mesoporous Mater 77:1
5. Inagaki S (2004) Studies Surf Catal 148:109
6. Ogawa M (2002) J Photochem Photobiol C Photochem Rev 3:129
7. Ogawa M (1994) J Am Chem Soc 116:7941
8. Ogawa M Chem Commun 1149 (1996)
9. Melosh NA, Davidson P, Feng P, Pine DJ, Chmelka BF (2001) J Am Chem Soc 123:1240
10. Wang J, Tsung C-K, Hong W, Wu Y, Tang J, Stucky GD (2004) Chem Mater 16:5169
11. Melosh NA, Lipic P, Bates FS, Wudl F, Stucky GD, Fredrickson GH, Chmelka BF (1999) Macromolecules 32:4332
12. Tanev PT, Liang Y, Pinnavaia TJ (1997) J Am Chem Soc 119:8616
13. Mesa M, Sierra L, López B, Ramirez A, Guth J-L (2003) Solid State Sci 5:1303
14. Martin T, Galarneau A, Renzo FD, Brunel D, Fajula F, Heinisch S, Crétier G, Rocca J-L (2004) Chem Mater 16:1725
15. Huo Q, Feng J, Schüth F, Stucky GD (1997) Chem Mater 9:14
16. Yang SM, Coombs N, Ozin GA (2000) Adv Mater 12:1940
17. Lu Y, Fan H, Stump A, Ward TL, Rieker T, Brinker CJ (1999) Nature 398:223
18. Rao GVR, López GP, Bravo J, Pham H, Datye AK, Xu H, Ward TL (2002) Adv Mater 14:1301
19. Bore MT, Rathod SB, Ward TL, Datye AK (2003) Langmuir 19:256
20. Fu Q, Rao GVR, Ista LK, Wu Y, Andrzejewski BP, Sklar LA, Ward TL, López GP (2003) Adv Mater 15:1262
21. Anderson N, Alberius PCA, Pedersen JS, Bergström L (2004) Microporous Mesoporous Mater 72:175
22. Hampsey JE, Arsenault S, Hu Q, Lu Y (2005) Chem Mater 17:2475
23. Grün M, Lauer I, Unger KK (1997) Adv Mater 9:254
24. Schumacher K, Grün M, Unger KK (1999) Microporous Mesoporous Mater 27:201
25. Grün M, Unger KK, Matsumoto A, Tsutsumi K (1999) Microporous Mesoporous Mater 27:207
26. Schumacher K, Hohenesche CDFV, Unger KK, Ulrich R, Chesne AD, Wiesner U, Spiess HW (1999) Adv Mater 11:1194
27. Grün M, Büchel G, Kumar D, Schumacher K, Bidlingmaier B, Unger KK (2000) Stud Surf Sci Catal 128:155
28. Schumacher K, Renker S, Unger KK, Ulrich R, Chesne AD, Spiess HW, Wiesner U (2000) Stud Surf Sci Catal 129:1
29. Luo Q, Li L, Xue Z, Zhao D (2000) Stud Surf Sci Catal 129:37
30. Pauwels B, Tendeloo GV, Thoelen C, Rhijn WV, Jacobs PA (2001) Adv Mater 13:1317
31. Nooney RI, Thirunavukkarasu D, Chen Y, Josephs R, Ostafin AE (2002) Chem Mater 14:4721
32. Tendeloo GV, Lebedev OI, Collart O, Cool P, Vansant EF (2003) J Phys Condens Matter 15:S3037
33. Liu S, Cool P, Collart O, Voort PVD, Vansant EF, Lebedev OI, Tendeloo GV, Jiang M (2003) J Phys Chem B 107:10405
34. Walcarius A, Sayen S, Gérardin C, Hamdoune F, Rodehüser L (2004) Colloids Int A 234:145
35. Lebedev OI, Tendeloo GV, Collart O, Cool P, Vansant EF (2004) Solid State Sci 6:489
36. Tan B, Rankin SE (2004) J Phys Chem B 108:20122
37. Shimura N, Ogawa M (2005) Bull Chem Soc Jpn 78:1154
38. Schacht S, Huo Q, Voigt-Martin IG, Stucky GD, Schüth F (1996) Science 273:768
39. Yano K, Fukushima Y (2004) J Mater Chem 14:1579
40. Lin H-P, Mou C-Y (1996) Science 273:765
41. Lin H-P, Chen Y-R, Mou C-Y (1998) Chem Mater 10:3772
42. Imai H, Takahashi N, Tamura R, Hirashima H (2001) Langmuir 17:17
43. Yang H, Coombs N, Ozin GA (1997) Nature 386:692
44. Che S, Liu Z, Ohsuna T, Sakamoto K, Terasaki O, Tatsumi T (2004) Nature 429:281

45. Sakamoto Y, Kaneda M, Terasaki O, Zhao DY, Kim JM, Stucky G, Shin HJ, Ryoo R (2000) Nature 408:449
46. Stöber W, Fink A, Bohn E (1968) J Colloid Int Sci 26:62
47. Bogush GH, Tracy MA, Zukoski CF IV (1988) J Non-Cryst Solids 104:95
48. Bogush GH, Zukoski CF IV (1991) J Colloid Int Sci 142:1
49. Keene MTJ, Gougeon RDM, Denoyel R, Harris RK, Rouquerol J, Llewellyn PL (1999) J Mater Chem 9:2843
50. Kleitz F, Schmidt W, Schüth F (2003) Microporous Mesoporous Mater 65:1
51. Brunauer S, Emmett PH, Teller E (1938) J Am Chem Soc 60:309
52. Barrett EP, Joyner LG, Halenda PP (1951) J Am Chem Soc 73:373